108073

JPRS 82854

11 February 1983

19990106 067

China Report

SCIENCE AND TECHNOLOGY

No. 187

Reproduced From
Best Available Copy

FBIS FOREIGN BROADCAST INFORMATION SERVICE

17
55
A04

NOTE

JPRS publications contain information primarily from foreign newspapers, periodicals and books, but also from news agency transmissions and broadcasts. Materials from foreign-language sources are translated; those from English-language sources are transcribed or reprinted, with the original phrasing and other characteristics retained.

Headlines, editorial reports, and material enclosed in brackets [] are supplied by JPRS. Processing indicators such as [Text] or [Excerpt] in the first line of each item, or following the last line of a brief, indicate how the original information was processed. Where no processing indicator is given, the information was summarized or extracted.

Unfamiliar names rendered phonetically or transliterated are enclosed in parentheses. Words or names preceded by a question mark and enclosed in parentheses were not clear in the original but have been supplied as appropriate in context. Other unattributed parenthetical notes within the body of an item originate with the source. Times within items are as given by source.

The contents of this publication in no way represent the policies, views or attitudes of the U.S. Government.

PROCUREMENT OF PUBLICATIONS

JPRS publications may be ordered from the National Technical Information Service, Springfield, Virginia 22161. In ordering, it is recommended that the JPRS number, title, date and author, if applicable, of publication be cited.

Current JPRS publications are announced in Government Reports Announcements issued semi-monthly by the National Technical Information Service, and are listed in the Monthly Catalog of U.S. Government Publications issued by the Superintendent of Documents, U.S. Government Printing Office, Washington, D.C. 20402.

Correspondence pertaining to matters other than procurement may be addressed to Joint Publications Research Service, 1000 North Glebe Road, Arlington, Virginia 22201.

JPRS 82854

11 February 1983

CHINA REPORT

SCIENCE AND TECHNOLOGY

No. 187

CONTENTS

PEOPLE'S REPUBLIC OF CHINA

 [III - CC - 84]

ABSTRACTS

NORWAY ESTABLISHING COMPUTER INSTITUTE

Oslo AFTENPOSTEN in Norwegian 25 Jan 83 p 12

[Article by Knut Løvstuhagen]

[Text] Trondheim, 24 Jan--The Trondheim University Computer Center (RUNIT) and the industrial concern Norsk Data A/S have begun work on establishing a software technology center in the Chinese capital Peking. The project is the first based on an entirely new philosophy in the U.N. aid program. The first class of 30 Chinese will be admitted to the Peking institute this fall. The 2-year training program offered will be oriented toward students with university degrees in mathematics and electronics, AFTENPOSTEN is told by Kristen Rekdal, research chief at RUNIT. Seven million kroner of public funds has been allotted for the project.

The United Nations is conducting a number of aid projects in the People's Republic of China, partly with a view to getting training in data technology under way in that country. China has a screaming need for data technology personnel. There is beginning to be a shortage of money in the world organization, however, and to remedy that problem the United Nations has decided to try a new financing arrangement for technological aid projects: If a member country indicates its willingness to finance the project, that country will get the contracts connected with it. The United Nations, however, retains control over the project just as if it were going to be a multilateral undertaking.

"The establishment of the Peking institute is a guinea pig for the new arrangement," says Rekdal. "Together with Norsk Data we contacted the Ministry of Foreign Affairs to find out about the possibilities of financing. The mood was positive there; a proposal on the matter was inserted in the 1983 budget and was approved by the Storting last month."

The 7 million kroner that has been appropriated for the project will cover supplies of computer equipment, training, and consulting work in connection with the founding. Norsk Data will supply the machine equipment and see to it that the Chinese learn to use it, while RUNIT will work out a training plan and give a series of courses with instructors taken from its own ranks and from the Norwegian Technical University. The Norwegian commitment will be for 3 years for the time being.

This project may prove very valuable both for Norsk Data and for RUNIT. The Chinese are out to buy computer technology, and they are therefore interested in professional contacts and training connected with such procurement. "On the whole it is difficult to overestimate the importance of the contacts that we are now making in China," Rekdal emphasizes. "The need for computer equipment and technology in that country is enormous. There is little domestic production, and the Chinese-made equipment is in some cases up to 15 years behind us in stage of development. But in certain small areas the Chinese are well ahead, so that they have a technological infrastructure that they can build upon. And although China has too little foreign exchange reserve to be able to import computer technology in such amounts that the imports can take care of the domestic demand, they can still buy abroad to cover certain key fields and to study the technology. For a little country like Norway even this little market is big and of considerable interest. Moreover, politically Norway is in a very good position in regard to China--a thing that can come to be significant for the further development of data-technology connections," says Rekdal.

Norsk Data and RUNIT will thus be in on establishing and starting up the software technology institute in Peking and will contribute with equipment, training, and instructional staff. But the intention from the outstart is that the Norwegian participation will gradually become superfluous, that the Chinese will in time become self-sufficient at the institute.

Norsk Data has already supplied computer equipment to China independently of the Peking project. In the fall of 1981, for example, a contract was signed for supplying a Type ND-500 computer, an installation of such high performance that for a time there were problems with getting an export license. NATO and the United States had to approve such an export. Norsk Data now has an application in for an export license for the same type of machine, and the Chinese have indicated an interest in additional equipment. These contracts have come about primarily as a result of the good contacts that research chief Rekdal of RUNIT has established in China.

8815
CSO: 3639/57

HIGH-ALTITUDE BALLOONS NOW PERFORMING VARIETY OF TASKS

Missions Enhance Space Astronomy Goals

Beijing GUANGMING RIBAO in Chinese 15 Oct 82 p 2

[Article and photo provided by the Atmospheric Institute: "China's First Astronomical Far Infrared Observations by High-Altitude Scientific Balloon Successful"]

[Text] Recently, the Shanghai Astronomical Observatory of the Chinese Academy of Sciences successfully utilized a high-altitude scientific balloon to conduct astronomical far infrared observations of the sun. The success of these observations demonstrates that China's astronomy has begun to enter the era of modern space astronomy.

The high-altitude scientific balloon is an important vehicle for space exploration. It is widely used for observation and experimental research by many disciplines such as high energy celestial physics, cosmic rays, atmospheric physics, atmospheric chemistry, infrared astronomy, remote sensing, space biology, physiology. At the same time, it is used a lot in test flights of space navigation instruments and equipment.

China began research in high-altitude scientific balloons in 1978. Led by the Earth Sciences Department of the Chinese Academy of Sciences, High Energy Physics Institute, Atmospheric Physics Institute, the Space Center, the Guangzhou Electronic Technology Institute, and the Shanghai Observatory jointly organized a balloon technology group and, in cooperation with related units, established a high-altitude scientific balloon technology system. Several dozen balloon engineering test flights have been conducted and at the same time balloons have been utilized to conduct a number of scientific observations; they have observed the gamma ray energy spectrum, the background of atmospheric neutrons, solar far infrared radiation, atmospheric wind fields in the stratosphere and gathered much valuable scientific data.

Space Observation Platform Carried Aloft

Kunming YUNNAN RIBAO in Chinese 23 Oct 82 p 3

[Article: "China Has Established a System of High-Altitude Scientific Balloon Technology"]

[Text] China has self-reliantly and rapidly established a high-altitude scientific balloon technology system, and has successfully sent a space science observation platform carrying various types of observational devices to altitudes of over 30 kilometers. It has provided an important technical means for space science research.

Among the carriers of artificial earth satellites, space probe rockets and balloons, the balloon has its outstanding advantage. Our nation spent 4 years of efforts and has released 28 large balloons with a volume in the 10,000-cubic-meter class. Some high-altitude scientific balloons have already developed a practical function in scientific research. This year, we successfully carried out observations of far infrared rays of the sun and cosmic gamma rays. They have enabled our nation's astronomy to progress in space and astronomical observation.

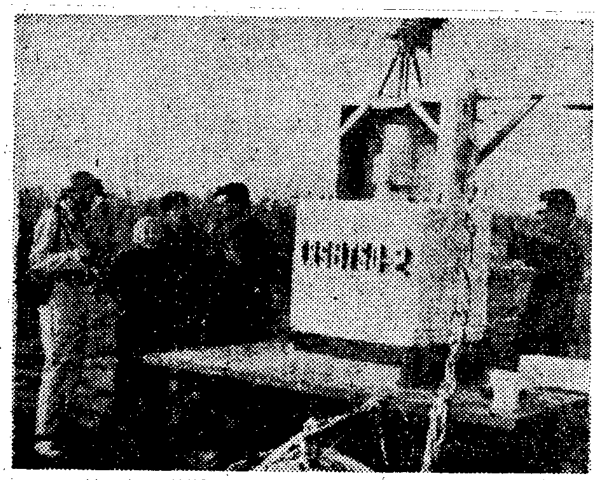

Famous physicist He Zehui [0149 3419 1979] (second from left) inspects research work at the balloon launching site of the Xianghe Atmospheric Physics Comprehensive Observatory in Hebei Province.

9296
CSO: 4008/31

ORE PROSPECTING IN LIAONING PROVINCE REVIEWED

Beijing TANKUANG GONGCHENG [PROSPECTING ENGINEERING] in Chinese No 5, 1982 pp 17-18

[Article by Liu Junpeng [0491 0193 7720]: "Selected Items of Engineering Experience in Ore Prospecting in Liaoning Province; Brief History of Drilling and Prospecting"]

[Text] For 28 years, under the leadership of the party, prospecting work by the Liaoning Bureau has realized great achievements and has developed greatly. At present, there are 6 comprehensive geological brigades, 2 hydrogeological brigades, 1 drilling and prospecting brigade, 1 pit prospecting brigade, a total of 10 ore prospecting brigades.

Over the past 28 years, they have completed [drilling] a total of 2,506,641 meters. In 1977, the highest number of drilling machines in operation was 90 units, annual progress reached a maximum of 214,419 meters in 1976. The monthly efficiency per unit reached a high of 427 meters in 1980. More than 20 mineral and underground water resources were prospected, including iron, copper, hard lead, pyrite, manganese, gold, molybdenum, mercury, arsenic, boron boron, phosphorus, limestone, asbestos, talcum, fluorspar, kaolin, coal, uranium, diamond, clay, zeolite. They have made their own contributions to the geological ore prospecting of the Liaoning Bureau.

For over 20 years, prospecting work by the Liaoning Bureau possessed the characteristic that the work always centered around hard rock strata; most of the mining regions worked had been hard rock strata, therefore, shotboring became the basic method of drilling by our bureau. In 1972, we began using diamond drills and this gradually became the key method of drilling and prospecting work. The course of development of drilling and prospecting work by our bureau can generally be divided into three stages.

I

The first stage was from 1953 when the bureau was founded to 1964. There were three characteristics during this period:

1. Production efficiency was not high and the technical level was low;

2. We engaged in technical renovation in a big way and the operations underwent great changes.

3. Three types of core removal drills appeared and core removal techniques developed greatly.

(I) In 1953 when the bureau was founded, we operated 14 drilling machines, the monthly efficiency per unit was 114 meters. By 1964, we were operating 39 drilling machines, and the monthly efficiency per unit was 264 meters. Production developed and efficiency improved. But the production level during this period was low. This was because just after establishing the bureau, drilling and prospecting had just started, workers were all new hands, they did not understand technology, they were unfamiliar with operations and technical equipment and the technological methods were backward.

(II) During the latter part of the 1950s, people's thinking was liberated, and we began to carry out technical renovations in a big way. We dared to rebuild hand held drilling machines and made some improvements. On the basis of the efforts of the workers and by learning from foreign experience, we mechanized operating procedures in a big way. By the beginning of the 1960s, we successfully popularized and renovated six new types of machinery, the hand cranked feeder, the ball chuck, the pipe twister, the ball chuck drawer, the vertical column pipe layer, and the movable work platform. They greatly improved operations, reduced labor intensity, and reduced or avoided personal accidents. These new machines are still being used in production now and they are serving a good function.

(III) At the beginning of the 1960s, our bureau continued to develop three new types of core removal drills. The Yingkou Geological Brigade was the first to successfully test and renovate the bent tube dual pipe reverse cycle alloy jet drill. Later, it also developed the single tube steel bit reverse cycle jet drill. This is an achievement in renovation that has a widespread significance. It solved the problem of the low extraction rate in soft and brittle geostrata and the problem of the low extraction rate in hard and brittle geostrata that had not been solved for a long time. To solve the problem of wear in drilling and prospecting asbestos at a certain asbestos mine, the pressed chuck type dual tube drill was developed. To solve the problem of contamination of talcum by slurry in drilling at a certain talcum mine, a piston type double tube drill was successfully renovated. The development and effective use of these three types of core extracting drills are a major development in our nation's drilling and core extracting technology and they have expanded the types of ores to be prospected in drilling and prospecting work.

II

The second stage was from 1965 to 1976. This period had 5 characteristics:

1. Start of a great increase in production efficiency;

2. The hand drill was rebuilt and renovated;

3. Transport and moving of drilling machines were mechanized.

4. The diamond drill became widely used.

5. Jet stream percussion rotary drill first developed successfully.

(I) Earlier, the hourly efficiency of drilling improved after the steel bit drill was popularized, but because the drilling rule was short, the efficiency of the steel bit could not be fully developed. In 1965, we learned to popularize the experience of "forced drilling" used in foreign nations. The results were good, and the hourly efficiency generally improved by more than 30 percent, and this was welcomed by the workers. To adapt to the technological needs in forced drilling, our bureau rebuilt an old drilling machine and the results were good. In 1969, we began to rebuild drilling machines in batches. By 1971, we completed the task of rebuiling all 110 drilling machines. This greatly influenced production in drilling and prospecting by the whole bureau. Accidents involving drilling machines were greatly reduced, the rules of operation for the forced drilling machine were smoothly popularized and this fully developed the efficiency of the shotdrilling and production efficiency rose greatly. The monthly efficiency per unit in 1965 was 288 meters. By 1976, this reached 388 meters.

(II) After rebuilding the 500-meter hand drill, we organized forces in 1972 to design and manufacture the open and closed type hydraulic oil rotary chuck drill. By 1976, 116 units had been manufactured. The drills of the whole bureau were replaced. The characteristic of this type of drill is that its center of gravity is low, its structure is simple, it is durable and easy to use, and it served an important function in production.

(III) At the beginning of the 1970s, our bureau's work in moving and transporting drilling and prospecting materials were quickly mechanized. We used the Dongfanghong tractor and the "mountain climbing tiger" (the material gathering model 50 tractor) to transport and move drilling and prospecting equipment and ship daily production materials. They not only improved efficiency, they also improved operating conditions.

(IV) Our bureau began in 1972 to use diamond drills and by 1976, we had 6 units. Diamond drilling during this period was a training period. We did not understand and we were unfamiliar with the technology but we progressed while exploring, therefore the results were not ideal enough. Of course, under certain favorable conditions, they can still manifest their superiority. For example, the drilling efficiency in hard and complete rock strata was high. In 1976, the monthly unit efficiency in drilling phosphorus ore by the Eighth Brigade reached 1,024 meters. That brigade used the XU600-2 model drill which also drilled holes reaching 1,214 meters deep. But, in general, there were many problems, and progress in drilling was slow, the cost was high, and complex rock strata could not be drilled, etc.

(V) The Ninth Brigade began to develop the jet stream percussion rotary drill in 1971. Preliminary results were obtained with the guidance and help from the Shenyang Electrical Machinery Academy at the beginning, later the brigade

developed and tested the drill on its own and realized great progress. On this basis, it cooperated with the Changchun Geological Academy and successfully developed the drill. The Ministry of Geology organized a technical evaluation meeting in 1979.

III.

The third stage is the period from 1977 to the present time. This period has five characteristics:

1. Diamond drilling technology and production efficiency visibly improved;

2. Protective hole plugging technology developed and improved greatly;

3. The LN54 model hydraulic ram was successfully developed and tested;

4. Labor organization and management methods improved;

5. A number of new technologies, new drilling tools, new machines were popularized and renovated.

(I) Since 1976, diamond drilling technology and production efficiency gradually improved visibly. This has been a period of development and improvement. By 1981, 14 diamond drills were in operation, constituting 50 percent of the rock core drills in operation. The monthly efficiency per unit was maintained at about 500 meters and it reached the highest of 519 meters in 1977. In 1978, the Shaomeng No 1 Brigade's 602 drill created a record of advancing 10,184 meters. The highest unit efficiency reached 1,133 meters.

Drill bit footage was improved. In 1979, the drill bit footage was 29.5 meters, in 1980 it was 34.6 meters, in 1981 it was 44.34 meters. This is a visible progress, and it was realized after implementing the method of rewarding efforts to conserve drill bits. The implementation of rewards for conserving drill bits greatly conserved drill bits, and at the same time, improved the level of the operating technique of workers. Now, we can say that we have basically realized "rational fitting of drills, careful operation, good maintenance." The workers' enthusiasm has been mobilized, and good economic benefits have been produced.

In recent years, the manufacturing quality of diamond drill heads has improved, the price has dropped, the cost of diamond drilling has dropped, and the cost per meter of some teams has dropped from over 70 yuan to over 30 yuan, approaching the cost of drilling by large caliber steel bit drilling. For example, some factories produce artificial diamond drill bits which given indentical hourly efficiency conditions, has a drill bit cost per meter drilled of only 5.5 to 6.7 yuan. This has enabled overall widespread use of diamond drills. We hope more factories can produce better and cheaper drill bits.

The work of outfitting equipment for diamond drilling is a problem our bureau has emphasized in solving some years ago. We have insisted on electrical motors as the power source of the drill. The BW250/50 pump was changed to a variable pump. We used the oil hydraulic ball chuck to overcome the

shortcoming of smoothing of the chuck rim. We used the small hexagonal drill rod, the small water joint, high pressure small guage water pipes, improved the durability of the equipment and the stability of the drill. We manufactured pliers for drill heads and used the ZY-10 model drilling pressure guage on an overall basis and such accessory devices. They provided smooth progress.

(II) At the middle of the 1970s, our nation's protective hole plugging technology realized new development. Our bureau gradually grasped some new protective hole plugging technology through learning, such as the use of polypropyrene amide low solidification phase mortar, polypropyrene amide washing liquid, and cement mortar grouting. They enabled us to better overcome difficulties in drilling complex geostrata. The application of these new technologies is a major manifestation of the improvement in the technical level of drilling and prospecting by our bureau.

(III) After the successful development of the jet stream percussion rotary drill, the Ninth team again successfully developed the LN54 model hydraulic ram. The outstanding advantage of this ram is that its operating stability is good and it is durable. In 1982, we are prepared to expand its tests.

(IV) We have popularized and renovated successfully a group of new technologies, new machinery and new drills. Beginning in 1981, we operated 2 cable core extracting drills and obtained preliminary success. The First Hydrological Team used the tooth gear drill head to enlarge a hole in the Quaternary Period Strata. The efficiency was five times that of ordinary methods. The Seventh Team succeeded in using the core extraction technique of prospecting kaolin and realized superior quality and high efficiency. The Eighth Team and such units successfully renovated the self-locking ball chuck drawer and the magnet steel floating flowmeter. The Ninth Team successfully renovated the juxtaposed dual spout reverse cycle drill, the electrical moveable working platform, and the seal for the handle of the drill rod. The Sixth Team improved the slant correction technique and realized preliminary success.

(V) Our bureau began in 1978 to implement "four-three shift work", which improved worker morale. Starting from 1980, we began to "standardize machinery." In that year, 12 rigs were honored for "superior achievements in the effort to standardize machinery", and they were given monetary rewards and certificates. This year, we continue this effort. At the same time, some brigades also reorganized their internal organization and established an economic responsibility system. They all realized preliminary success and management level improved.

In general, in our bureau's drilling and prospecting work, the technical level and production efficiency have improved after many years of effort by all sectors, have basically met and satisfied the requirements of geological work, and have completed the various prospecting tasks well. In production level, the monthly efficiency per unit in 1979 was 403 meters. This was the first time that the efficiency has surpassed 400 meters. In 1980, the monthly efficiency per unit was 427 meters, the average annual progess of operating units was 4,103 meters, and the percentage of superior quality holes was 90.2 percent, creating the best levels ever for our bureau.

The above points simply state the situation in the development of production in drilling and prospecting by our bureau. They only included the achievements. There are still many problems. We must learn from sister bureaus and brigades to achieve more for geological ore prospecting.

9296
CSO: 4008/24

CONTENTS OF 'AERODYNAMIC HANDBOOK' OUTLINED

Beijing GUOJI HANGKONG [INTERNATIONAL AVIATION] in Chinese No 11, 5 Nov 82 pp 4-6

[Article by Zhao Xuexun [6392 1331 6064]: "Introduction to the Aerodynamic Handbook for Aviation (Part I)"]

[Text] The "Aerodynamic Handbook" is published and edited jointly by the Chinese Aviation Research Institute and the Chinese Aerodynamic Research and Development Center. It is intended to be a reference tool for aircraft designers and specialists from aeronautical institutions and research organizations. In preparing the handbook, the authors and editors tried to incorporate and exploit China's current scientific experience and achievements, and also presented several new methods; furthermore, through analyses and examples, an attempt was made to select, verify, and modify certain new results which were published abroad in the 70's.

The handbook is divided into four volumes. Its content includes notations, coordinate systems and specification of units; international standard atmosphere data; fundamental equations of aerodynamics and equations of motion. It also includes methods of calculating aerodynamic characteristics and flight performance for airplanes without attachments; the aerodynamic calculations are given for the following conditions: longitudinal and lateral, stationary and non-stationary, free-flight and near-ground, low speed and supersonic speed, and for scenarios ranging from small angle-of-attack, linear flow regime to large angle-of-attack, non-linear flow regime.

In order to facilitate calculations in engineering design, most calculations are given in terms of analytical formulas and system diagrams. Also, because of the increasing number of applications of computational aerodynamics in aircraft design, the handbook provides 10 computational and design programs which have been well established on China's commonly used computers.

Volume 1 of the handbook, which contains the fundamentals of aerodynamics, was published in 1975 by the Office of Science and Technology Intelligence of the Third Ministry of Machine Building; volume 2, which contains methods of calculating the longitudinal, stationary aerodynamic characteristics, will soon be published by the Defense Industry Publication Office; volume 3, which contains the method of calculating lateral derivatives and other special problems, is currently being written; volume 4, which contains the

methods of calculations in flight mechanics, has already been published in 1978 by the Defense Industry Publication Office. The highlights of each volume are presented in the following sections.

Volume 1: Fundamentals

This volume contains three chapters. In the first chapter, the notations, coordinate systems, and measurement units commonly used in aerodynamics and flight mechanics problems are specified, rigorous definitions of various important parameters are given. To facilitate the use of foreign materials, an appendix is included which contains comparisons and conversion charts between the standards used in this handbook and foreign standards, international standards, and international unit system.

Chapter 2 contains a complete collection of the fundamental equations and formulas of aerodynamics, as well as charts and diagrams of fluid parameters. Specifically, it includes the basic aerodynamic equations, and equations of fluid mechanics and thermodynamics in rectangular, cylindrical, and spherical coordinate systems. It also includes the velocity potential equations, the stream function equations, the characteristics equations, and other formulas, charts, and transition elements which relate fluid elements under commonly encountered conditions.

Chapter 3 contains the tables of standard atmosphere. The tables were systematically constructed on the basis of standard atmosphere data and practical considerations in airplane design. The altitude range in the table extends from 1,000 m to 32,000 m at 50-100 m intervals. It also includes tables of total pressure, total temperature, and dynamic pressure for altitude ranging from 0 to 32,000 m and Mach numbers ranging from 0 to 3.6. The altitudes are given at 1,000 m intervals and the Mach numbers are given at intervals of 0.1, 0.2, and 0.05 respectively.

Volume 2: Methods of Computing Longitudinal, Stationary Aerodynamic Characteristics

In this volume, the methods of computing the longitudinal, stationary aerodynamic characteristics of a "clean" airplane with no attachments are presented. The volume contains five sections which deal with the following topics: the airfoil, the wing, the fuselage, the wing-fuselage combination, and the wing-fuselage-tail combination. Each section is divided into units of aerodynamic characteristics and aerodynamic configuration, and is presented in loose-leaf format. A summary of each section is described below.

The Airfoil: This section contains 21 loose-leaf pages; its contents include airfoil data, methods of calculating the aerodynamic characteristics of airfoils, and methods of airfoil design. The airfoil data include more than 200 widely used NACA series airfoils, 5 groups of RAE series airfoils with relative thickness of 4-5 percent, and more than 20 TSAGI [Central Aerodynamic Institute: USSR] series airfoils which are commonly used on airplanes in this country. In addition, for the purpose of verifying numerical computation, several NLR research airfoils of the Dutch Aeronautical

Institute are also included. The NACA series include more than 20 airfoils with the basic mean lines of several families, more than 90 low-speed airfoils with relative thickness of 6-24 percent and high-speed airfoils with relative thickness of 2-21 percent, and more than 90 commonly used combination airfoils. Also, more than 90 high-speed airfoils generated by interpolation are included. In addition to the geometric data and pressure distribution data of the above airfoils, low-speed wind-tunnel data of more than 200 airfoils are presented. For the TSAGI, RAE, and NLR airfoils, geometric and pressure distribution data are presented.

In addition to the engineering methods for computing aerodynamic characteristics, two methods of calculating the pressure distribution of sub-critical flows are presented: the classical Theodorsen method, and the method of sources and sinks which is applicable for arbitrary two-dimensional airfoils. To meet the needs of transonic flow calculations, a method of conformal transformation and contact transformation for computing the pressure distribution of a blunt-nose, thick wing with arbitrary lift is presented. To facilitate high-speed computation in engineering applications, a method of relaxation using finite differences to solve the approximate velocity potential equations for transonic flow is presented; this method is limited to small angle-of-attack and thin airfoils, but it provides highly accurate results and requires little computation time.

The chapter on airfoil design information and methods contains a large amount of statistical data of current airplanes, and presents a detailed discussion of the standard airfoil matching techniques. To facilitate detailed airfoil design, a method based on the second order theory under sub-critical flow conditions is presented. The method can be used to design airfoils based on given pressure profile, or to design the camber distribution and the corresponding angle-of-attack based on pressure distribution on the upper surface and the airfoil thickness. For transonic airfoils, an approximate method is introduced for designing a closed airfoil based on given Mach number, pressure coefficient, and the coordinates of the wing circumference. Numerical examples show that at $M = 0.75$, the errors in the chord-wise and longitudinal coordinates are respectively 0.6 percent and 0.7 percent.

The Wing: This section contains 19 loose-leaf pages which deal with methods of calculating the aerodynamic characteristics of wings. A specific method is presented for computing the lift and pitching moment of ordinary planar wings with symmetric airfoils and zero twist; its accuracy is comparable to those reported in foreign literature. To supplement the method, several semi-empirical techniques applicable under special conditions are also included. In addition, this section presents the method of estimating the critical angle-of-attack and maximum lift coefficient. Compared with experimental results, the errors in the calculated maximum lift coefficients are less than 5 percent and 3 percent respectively for wings with large and small aspect ratios. Curves are presented for computing the viscous drag and wave drag; for computing the induced drag of a zero-twist planar wing in subsonic flow; and for computing the supersonic drag based on the theory of conical flows. To facilitate the use of wind-tunnel test data, a semi-empirical

formula is presented for correcting the test data of induced drag coefficient.

In order to calculate the aerodynamic characteristics of an arbitrary planar wing with arbitrary twist, a numerical procedure based on the theory of lifting surface of subsonic and supersonic thin wings (fundamental solution) is presented. It is applicable for a wing with a straight-line trailing edge and a leading edge represented by up to 3 straight-line segments. Accurate results in pressure distribution, lift, pitching moment, and induced drag can be obtained by dividing the wing into 120 segments.

The Fuselage: This section, which contains 17 loose-leaf pages, presents a method of calculating the aerodynamic characteristics of fuselages which is based primarily on the slender-body theory and large amount of experimental data; it can be used in the calculations for regular-shaped fuselages. For fuselages with irregular structures, a number of engineering techniques are recommended, and detailed numerical procedures are presented.

In the subsonic regime, the method of calculating lift and pitching moment can be used for angle-of-attack as large as 12-16°. The method can also be used in the transonic and supersonic regimes for relatively large angle-of-attack.

The drag of the fuselage is calculated separately for each type of drag. The surface frictional drag is calculated using the conventional equivalent flat-plate method. For the purpose of computing pressure drag (mainly wave drag), practical data sets are presented for various shapes of the nose (sharp nose, open nose, and 30° cone), and the tail (knife edge tail, and sharp tail), as well as for a nose-tail contour represented by a nth order power function (n=1-5); they include data sets of wave drag coefficients due to interference between the nose and the tail. This section also presents methods of estimating the base drag in the presence of a jet stream, and the wave drag of a cockpit cover.

In order to avoid computational errors due to simplification of the fuselage contour, numerical procedures are presented for calculating the subsonic and supersonic lift and drag of fuselages with arbitrary cross-section, camber and angle-of-attack. In addition, methods of computing the fuselage pressure distribution in subsonic and supersonic flows are also presented so that the actual pressure gradient can be estimated in detailed fuselage design.

Combined Configuration: This section contains 22 loose-leaf pages divided into two main parts: wing-fuselage configuration and wing-fuselage-tail configuration.

The aerodynamic characteristics of a wing-fuselage configuration depends primarily on calculating the interference factor. In this section, the conventional interference factor which applies only to a single mid-wing and cylindrical fuselage configuration is generalized to a combined configuration

with a twisted wing. It also presents a theoretical derivation of the interference factor for an elliptical fuselage and single mid-wing configuration, and gives an experimentally verified correction factor to account for the effect of non-circular cross-sections. In addition, a preliminary method of estimating the interference factor of other types of configurations is also presented.

In considering the effect of wingtip downwash on the characteristics of moments, a method of calculation which agrees closely with experimental results for both subsonic and supersonic flows is presented. Comparison with experimental results shows that the interference factor computed from this method has a relative error of 3-7 percent for small angle-of-attack; the error in the lift curve slope is $\pm$ 3 percent; and the error in the focal point is within $\pm$ 5 percent. Hence, it is superior to most conventional methods.

The aerodynamic characteristics of a wing-fuselage-tail configuration are calculated by first calculating the mutual interference between the individual components and then superposing the contribution of each component. In this section, an engineering method of estimating the downwash of a wing-fuselage configuration under subsonic, supersonic, and transonic conditions, and a method of estimating the velocity damping coefficient of a thick wing placed in the trails of a wing-fuselage configuration under subsonic and transonic conditions are presented. Comparison with experimental results shows that the relative errors are within 10 percent and 7 percent respectively. On the basis of the above analysis, a method of estimating the lift and the center of pressure of a horizontal tail is also presented.

At the present time, a rigorous method of calculating the drag characteristics of wing-fuselage configurations is not available. In this section, an approximate method based on the fundamental principles of physics is presented; it can be used to provide a first-order estimation of drag for combined configurations.

3012
CSO: 4008/35

Y-11 WINGTIP SAILS TESTS REPORTED

Beijing GUOJI HANGKONG [INTERNATIONAL AVIATION] in Chinese No 11, 5 Nov 82 pp 2-3, 23

[Article by Guan Ruizhang [7070 3843 4545]: "Test of Wingtip Sails on the Y-11 Agricultural Aircraft"]

[Text] In the 1980, No 1 issue of "International Aviation," we discussed the testing of wingtip winglets on the Y-11 agricultural aircraft. Recently, we have further conducted tests of wingtip sails on the same aircraft. The wingtip sails provided better aerodynamic performance than the winglets and were more effective in dispersing the wingtip vortices and in reducing the overall induced drag of the aircraft.

Basic Principle. The basic aerodynamic principle of the wingtip sails is similar to that of the wingtip winglets. During flight, the high pressure air below the wing flows around the wingtip in a spiral pattern, creating trailing vortices and producing induced drag. By installing winglets or sails on the wingtip, it is possible to suppress the spiraling flow and reduce the strength of the trailing vortices and hence the induced drag. However, the direction of the flow field near the wingtip is highly variable; if only one winglet is installed, its camber and twist must be carefully designed to accommodate the wide range of local flow deflection angles; otherwise, its aerodynamic benefits cannot be fully achieved. The wingtip sails are essentially multiple winglets installed at different positions of the wingtip according to the characteristics of the local flow field; hence the aerodynamic efficiency is much higher. Figure 1 shows a schematic diagram of the flow field of three wingtip sails. The sails not only generate thrust from side wind like the sails on a sail boat, but also "comb" the spiraling air flow from the wingtip into uniform flow, like fixed fan blades. Furthermore, they are more effective than the winglets in dispersing the wingtip vortices.

Installation of the Sails. It can be seen from Figure 1 that the streamlines at the wingtip are in the form of spirals; thus, the sails must be interleaved, and positioned according to the spiraling streamlines. Figure 2 shows a typical arrangement of the sails. The angle between the two sails Θ (tentatively called the spiral angle) should be chosen as large as possible based on wind tunnel tests. Since each sail produces not only lift but also

its own downwash, the spiral angle should not be so small that one sail is submerged in the downwash of other sails; otherwise, it will result in reduced lift, increased drag, and premature flow separation over the sail.

Length of the Sail. Figure 3 shows the measured flow field around the wingtip. For a given angle of attack α, the ratio between the local wingtip flow direction ϕ and the angle of attack, ϕ/α, decreases rapidly with increasing distance from the upper surface. If the sail is too long, portions of the sail may be outside the disturbance flow field; in this case, the sail not only produces no additional lift, it contributes part of its frictional drag. The length of a sail is primarily determined by the angle of attack of the wing. For large angle of attack (e.g., 10°), the length should be 0.41 times the wingtip chord length; for small angle of attack (e.g., 6°), it should be 0.30 or even 0.24 times the wingtip chord length. The shape of the sail is generally a trapezoid with a taper ratio of 0.5; the base chord is 0.16 that of wingtip chord length.

Airfoil Type of the Sail. In a complicated disturbance flow field, a high-lift, low-drag airfoil should be chosen for the sail design; this not only provides good aerodynamic performance under design conditions, but also prevents flow separation under non-design conditions. For example, one can use the GA(W)-1, GA(W)-2 or GU airfoils, or the NACA6 series symmetric airfoils such as the NACA 630212. To ensure that flow separation does not occur, the airfoil shape near the sail tip should have little or no camber; the camber should increase toward the base of the sail.

Skim Angle of the Sail. The skim angle of the sail is the angle between the base chord of the sail and the wing chord (the angle τ in Figure 2). This angle actually determines the operating angle of attack of the sail. Since each sail is located in a different part of the flow field, its skim angle is also different; the outside skim angle is considered to be positive. The first sail has the largest skim angle, subsequent sails have progressively smaller angles. It can be seen from Figure 3 that close to the wing surface, the angle ϕ is largest near the leading edge. Therefore, increasing the skim angle will reduce the local angle of attack at the intersection of the sail and the wing, and prevent flow separation at the base of the sail.

Tilt Angle of the Sail. The angle β between the surface of the sail chord and the surface of the wing chord is defined as the tilt angle. The β angle of each sail should be different from others so that no one sail will be in the trails of the others. Other considerations for selecting different β angles are lateral stability of the aircraft and prevention of boundary layer separation, etc. In general, β for the first sail is zero ($\beta_1=0°$), and increases progressively for subsequent sails. The angle between two adjacent sails should be in the range between 15° and 20°. Experimental results from abroad show that for a fixed number of sails, the smaller the tilt angles, the more effective they are in reducing induced drag.

Twist Angle of the Sail. Figure 3 also shows that in the vicinity of the upper wing surface, the angle ϕ can be as large as 4 times the angle of

attack; but at a distance only 0.2 chord length above the wing surface, ϕ decreases to less than 0.5 times the angle of attack. In order to avoid flow separation at the base or to improve the aerodynamic performance of the wingtip, the sail must be designed to have a certain aerodynamic twist. If the sailtip cross-section is considered as a reference, and a linear variation is assumed, then the base cross-section will have a negative twist angle, which can be as large as -20°.

The Number of Sails. In principle, the effectiveness of induced drag reduction improves with increasing number of sails. But each sail produces lift as well as frictional drag and induced drag. A large number of sails not only increases frictional drag but also creates more interference between the sails; some sails will inevitably be submerged in the trails of others, and partial separation of the boundary layer will take place, thereby degrading the aerodynamic performance of the sails. For example, the experimental results from abroad show that for sails equal to 0.24 times the chord length, the lift-to-drag ratio decreases drastically with increasing number of sails; there is essentially no improvement in performance beyond 3 sails. However, with longer sails, 4 sails may be used.

England began research work on the wingtip sail in 1978. They conducted low-speed wind-tunnel tests of wingtip sails on a 1/7th scale model of the "PARIS" aircraft. Under the condition of $\alpha=6°$, $C_L=0.5$, the induced drag of the aircraft was reduced by 12 percent by installing just 1 wingtip sail; with 3 sails, the induced drag was reduced by 28 percent, and the lift-to-drag ratio increased by 25 percent. Subsequent flight test results showed that by installing one sail on each side, the induced drag was reduced by 9 percent, and when 3 sails on each side were installed, the induced drag was reduced by 29 percent. By comparison, with wingtip winglets, the maximum reduction in induced drag was 20-25 percent (KC-135), and on the DC-10, it was only 12 percent. In 1979, flight tests were again conducted to study the fuel consumption and control performance of the "PARIS" MS760 aircraft. With 3 sails installed on the wingtip, the induced drag was reduced 27 percent when the lift coefficient was 0.22. Because of the reduced total drag, a fuel saving of 4.5 percent can be achieved under the standard lift coefficient of $C_L=0.35$, and a 11 percent fuel saving when $C_L=0.8$. The pilot noticed a substantial increase in the climb rate during take-off. With increasing number of sails, there was essentially no change in the role damping control of the flap.

In 1981, we conducted tests of wingtip sails on the Y-11 aircraft in a 4X3 m^2 low-speed wind tunnel. The sails were of trapezoidal shape with a taper ratio of 0.5; the lengths of the sails were respectively 0.41 times wing chord (long sail) and 0.24 times wing chord (short sail). The long sails used the GU airfoil design, and the short sails used both NACA0012 and GU designs. The twist angles of the sails were respectively 12° (long sail) and 7° (short sail). Attempts were also made to determine the optimum combination of tilt angle, skim angle, and the number of sails. The test results indicate that by installing 4 sails on the Y-11 wind tunnel model, the slope of the lift curve increased by 9 percent. With flaps deflected

(considering ground effect), the maximum lift coefficient increased by 5 percent. The maximum lift-to-drag ratio of the aircraft increased by 9.7 percent, and the induced drag under nominal lift coefficient condition decreased by 20 percent. The tests also indicate that the sails had little effect on lateral stability. Typical test results are presented in Figure 4 and Figure 5.

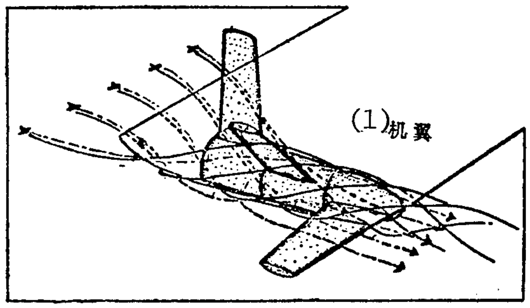

Figure 1. Flow Field Around Wingtip During Flight and Wingtip Sails (The dotted lines are streamlines without sails, and the solid lines are streamlines with sails.)

Key:

1. Aircraft wing

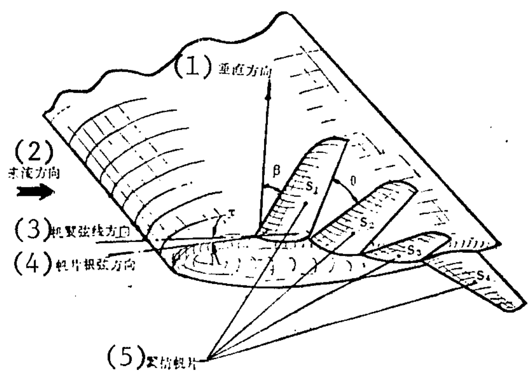

Figure 2. Schematic Diagram Showing the Installation of Wingtip Sails

Key:

1. Vertical direction
2. Direction of airflow
3. Direction of wing chord
4. Direction of the base chord of the sail
5. Wingtip sails

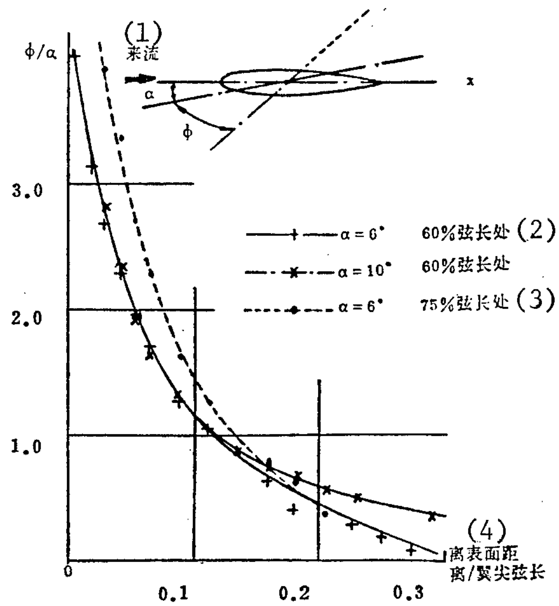

Figure 3. Measured Results of Wingtip Flow Field

Key:
1. Air flow
2. At 60 percent chord length
3. At 75 percent chord length
4. Distance from the surface/wingtip chord length

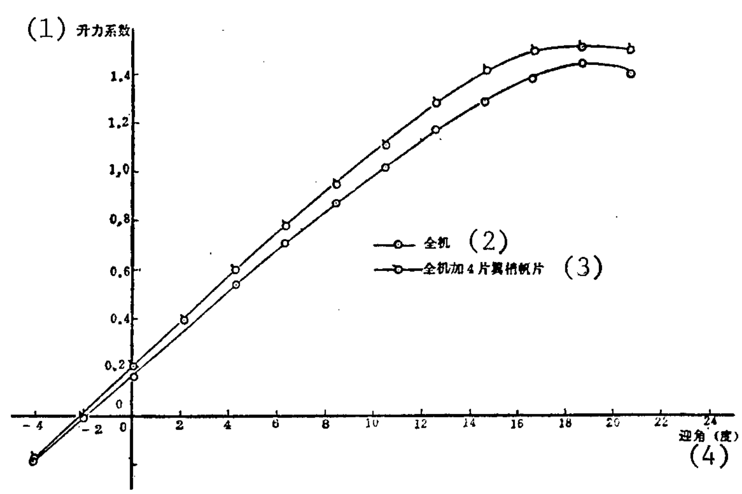

Figure 4. Effect of Sails on the Lift Characteristics of the Y-11 Aircraft

Key:
1. Lift coefficient
2. Entire aircraft
3. Entire aircraft with 4 wingtip sails
4. Angle of attack (degrees)

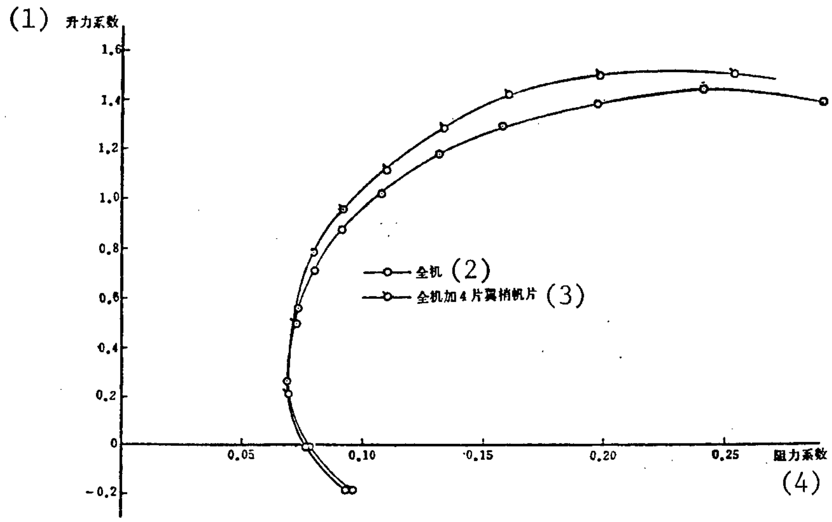

Figure 5. Effect of Sails on the Lift-to-Drag Ratio of the Y-11 Aircraft

Key:

1. Lift coefficient
2. Entire aircraft
3. Entire aircraft with 4 wingtip sails
4. Drag coefficient

3012
CSO: 4008/35

PROTECTING AIR RAID SHELTERS AGAINST PENETRATING RADIATION

Chongqing DIXIA GONGCHEN [UNDERGROUND ENGINEERING] in Chinese No 8, 1982 pp 25-32, back cover

[Article by Kang Ning [1660 1337]: "Calculations for the Protection of Air Raid Shelters Against Penetrating Radiation"]

[Text] The fundamental elements that constitute the cause of injury by a nuclear explosion are shock waves, light radiation and nuclear radiation. When a nuclear device explodes in the atmosphere below an altitude of 30 kilometers, the energy of light radiation constitutes 35 percent of the total energy of the explosion while 50 percent of the energy of nuclear fission is consumed in the formation of shock waves, and the remaining 15 percent of energy is released in the form of nuclear radiation. Although the energy of nuclear radiation constitutes only a small portion of the total energy of a nuclear explosion, because it has a very strong penetrative ability, therefore, it can cause injury at a very far distance from the center of explosion and even inside shielded areas. Thus, studying calculations for the protection against nuclear radiation is a difficult task of technical personnel in underground engineering.

Calculations for the protection of underground structures against nuclear radiation include three parts, the roof (covering), walls and holes. The penetrating dose must not surpass the allowable dose (50 roentgens). But in currently available reference works, this problem lacks a clear exposition, and there are still questions in the calculations worth deliberation. Most consider only the penetrating radiation in the direction along the normal line of nuclear radiation and do not consider oblique penetration of nuclear radiation. Although some have taken oblique radiation into consideration, they have not considered oblique radiation after the smoke cloud rises into the atmosphere. This article presents some opinions aimed at the above situation, addresses the question of protecting underground structures from nuclear radiation and invites comments from readers.

I. Characteristics of Nuclear Radiation (Penetrating Radiation) and Attenuation of Radiation

1. General Characteristics of Penetrating Radiation

Nuclear radiation consists of α particles, β particles, γ ray and three types of neutron streams. The effective range of α particles in air is only several centimeters, the effective range of β particles (high velocity electrons) in air is also only several meters. The range of γ ray (high energy electromagnetic radiation similar to X ray) in air reaches several thousand meters. The range of neutrons (particles released by nuclear fission and fusion) in air is several hundred meters. It can be seen that the calculation of penetrating radiation is mainly to study the calculation of γ ray and neutron streams.

But, in actual structural calculations, we do not consider all the γ ray and neutron streams released by an explosion of a nuclear weapon. In an explosion of a nuclear fission bomb, γ radiation can be divided according to the duration of emission into instantaneous γ radiation, short-lived γ radiation and γ radiation measured in seconds. Research shows that the dose of radiation in the explosion area is mainly the radiation measured in seconds followed by short-lived radiation. Their longest duration of irradiation on ground surface targets is 15 to 20 seconds. Neutrons released by nuclear fission can be divided into fast neutrons, medium velocity neutrons and slow neutrons. Because the dosage of slow neutrons is smaller than the dosage of fast neutrons inside the area of injury by penetrating radiation, and at the same time because neutrons are released within a relatively short time, injury by neutrons is usually caused by fast neutrons. Without doubt, in calculating protective structures, consideration is only given to γ radiation measured in seconds, short-lived γ radiation and fast neutrons. The dosage of penetrating radiation released by a fusion bomb (thermonuclear bomb) not only includes γ ray and fast neutrons, it also includes some ultrahigh velocity neutrons.

2. The Process of Attenuation of Penetrating Radiation (see pages 26 and 27)

II. Calculating the Protection of Underground Structures Against γ Ray

1. Calculating the Protective Layer (including the cover and walls)

The intensity of the γ ray transmitted from the center of explosion to the underground structure continues to attenuate as the ray passes through the protective layer and enters the interior of the underground structure because of the mutual action of its atoms (there are photoelectric absorption, Compton-Wu Youxun [0702 2589 6064] scattering and electron-position pairs) (Refer to p 33 in "γ Radiation in an Atomic Explosion"). When the incident γ ray is perpendicular, its computational formula is:

$$D_{\gamma} = D_{\gamma 0} \quad K = \alpha_{\gamma} D_{\gamma 0} e^{-\mu x} \tag{1}$$

where: D_{γ} - the dosage of γ radiation through the protective layer (roentgen);

$D_{\gamma 0}$ -- dosage of incident γ radiation (roentgen);

e -- Naperian base of natural logarithm;

μ -- The coefficient of total attenuation of γ radiation due to the protective layer as listed in Table 1;

α_γ -- The coefficient of attenuation of the softest scattering inside the protective layer considered, as indicated in Figure 1;

K -- Coefficient of attenuation of the dosage of γ radiation due to the protective layer;

x -- Thickness of the protective layer (centimeter).

Table 1

Name of materials	Effective attenuation coefficient μ (centimeter^{-1})	
	ε_0 = 1 mega electron volt	ε_0 = 2 mega electron volts
Wood	0.033	0.027
Soil	0.08	0.05
Concrete	0.11	0.07
Iron	0.33	0.25
Lead	0.80	0.39
Remark	ε_0 - energy of photons	

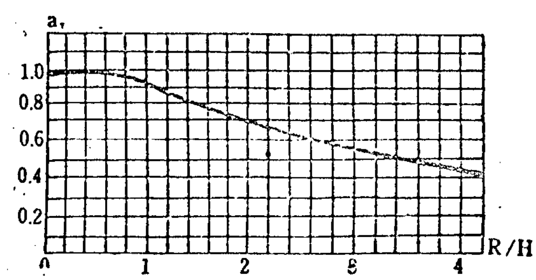

Figure 1. The α_γ of Soil and Concrete Varies With R/H

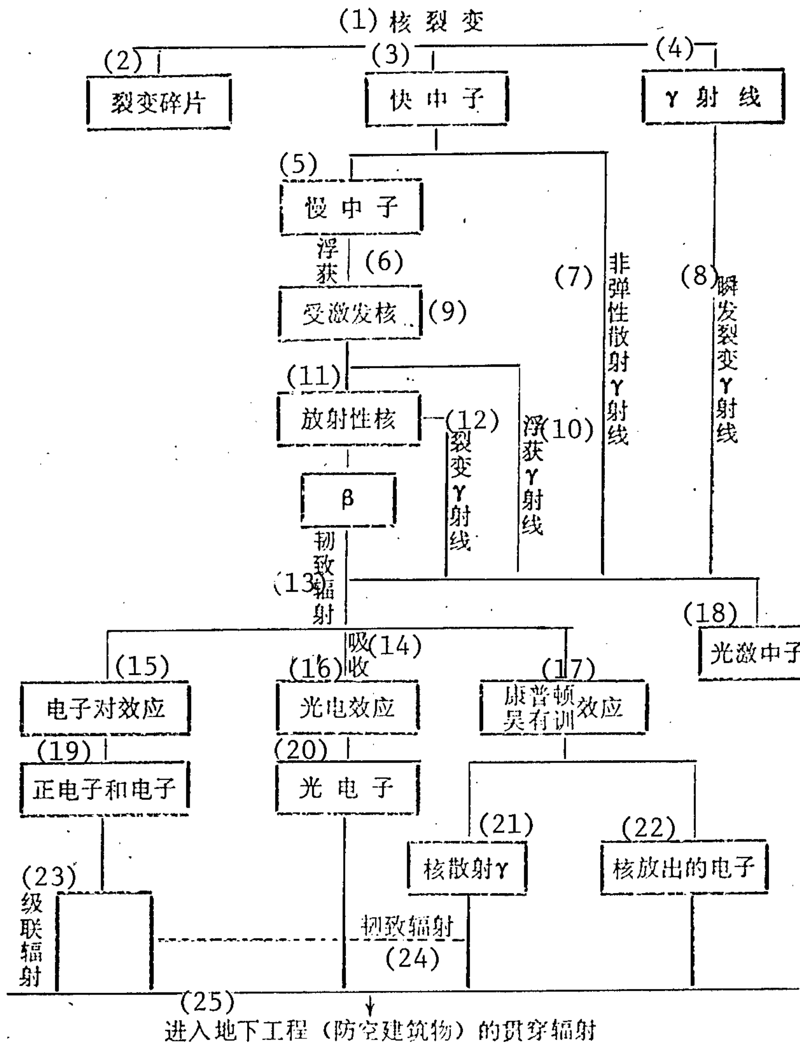

Key:

(1) Nuclear fission
(2) Fission fragments
(3) Fast neutrons
(4) γ ray
(5) Slow neutrons
(6) Capture
(7) Nonelastic scattering γ ray
(8) Instantaneous fission γ ray
(9) Excited nuclei
(10) Captured γ ray
(11) Radioactive nuclei
(12) Fission γ ray
(13) Pliable radiation
(14) Absorption
(15) Electron pair effect
(16) Photoelectric effect
(17) Compton-Wu Youxun [0702 2589 6064] effect
(18) Light excited neutrons
(19) Positrons and electrons
(20) Photoelectrons
(21) Nuclear scattering γ
(22) Electrons released by the nuclei
(23) Cascade radiation
(24) Pliable radiation
(25) Penetrating radiation entering the underground structure (air raid shelter)

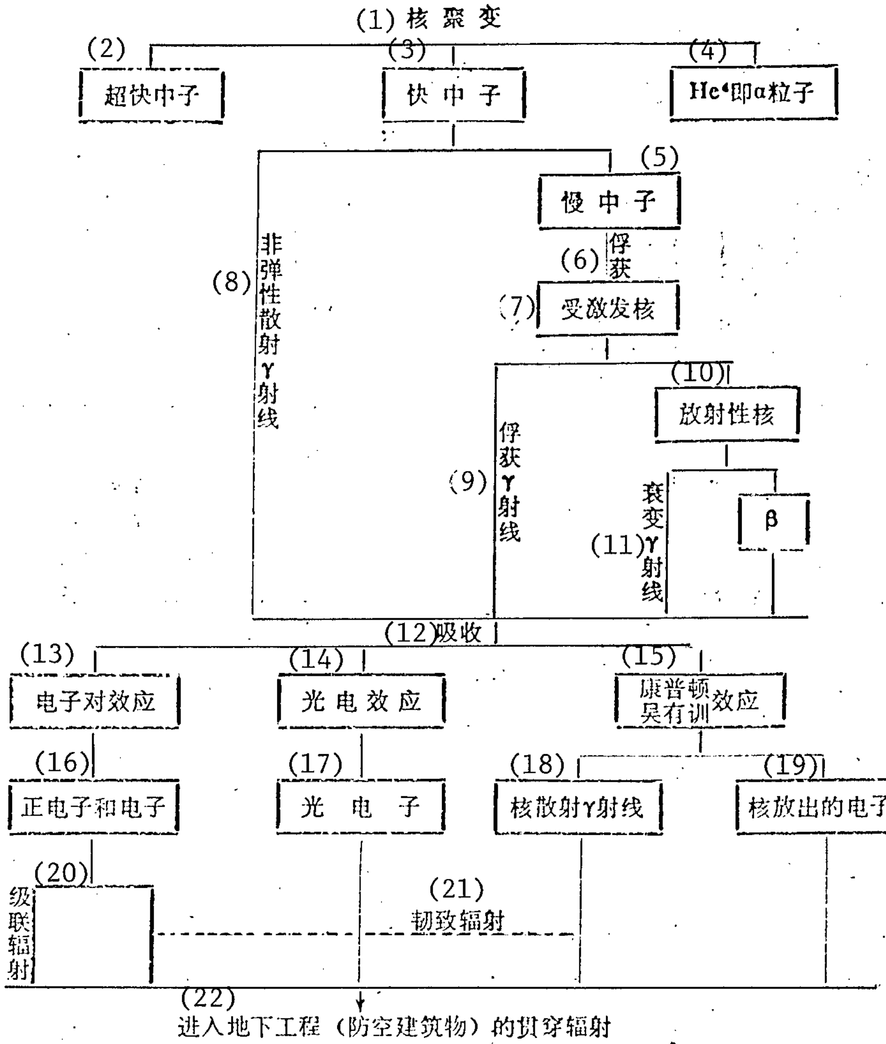

Key:

(1) Nuclear fusion
(2) Ultrahigh velocity neutrons
(3) Fast neutrons
(4) He^4 i.e., α particles
(5) Slow neutrons
(6) Capture
(7) Excited nuclei
(8) Nonelastic scattering γ ray
(9) Captured γ ray
(10) Radioactive nuclei
(11) Decaying γ ray
(12) Absorption
(13) Electron pair effect
(14) Photoelectric effect
(15) Compton-Wu Youxun [0702 2589 6064] effect
(16) Positrons and electrons
(17) Photoelectrons
(18) Nuclear scattering γ ray
(19) Electrons released by the nuclei
(20) Cascade radiation
(21) Pliable radiation
(22) Penetrating radiation entering underground structure (air raid shelter)

In the case of oblique incidence, attenuation of intensity γ ray is more rapid than that of the ray incident upon the protective layer along the normal direction (i.e., perpendicular incidence). This is because the γ ray has to travel a longer distance, i.e., the thickness of the protective layer in the direction of the beam of the ray increases in relation. According to O.I. Leipunski, at this time, the coefficient of attenuation K_γ of the dosage in formula (1) can be expressed by the following formula:

$$K_\gamma (1, \psi, \varepsilon_0) = a(\psi, \varepsilon_0, K) K_\gamma (1, \varepsilon_0) \tag{2}$$

where: $K_\gamma (1, \varepsilon_0)$ - includes the coefficient of attenuation of the dosage when a γ ray with a photon energy ε_0 along the normal line penetrates a protective wall of thickness 1, calculated by

$$K = e^{-\mu x} = 2^{-x/d};$$

$a (\psi, \varepsilon_0, K)$ -- coefficient taking oblique incidence into consideration (Table 2).

When the angle of incidence is between 0 and 30°, we can regard $a(\psi, \varepsilon_0) = 1$, i.e., the oblique thickness and the perpendicular thickness of the protective wall as equal.

Everyone knows that the radioactive cloud (γ radiation is the main source of radiation) formed after an atomic explosion rises at a fixed velocity. (ν_{cp} = 72 - 100 meters/second). The dosage of radiation of γ ray acting upon the protective layer of the fortification and the minimum thickness for penetrating the protective layer continually change. Radiation from different angles of inclination acts differently upon the protective layer. The smaller the angle of inclination, the larger the relative thickness and the thinner the relative thickness of the wall. Conversely, the larger the angle of inclination, the thinner the relative thickness of the cover and the greater the relative thickness of the wall (Figure 2).

At this time, the dosage of γ radiation attenuating through the protective layer can be calculated according to the following formula:

$$D_\gamma = \sum_{i=1}^{n} \frac{a_\gamma D_{\gamma 0}}{n} a_i(\varphi_\gamma, \varepsilon_0, K) e^{-\mu x_i} \tag{3}$$

Expressed in half-value thickness:

$$D_\gamma = \frac{a_\gamma D_{\gamma 0}}{n} \sum a_i(\varphi, \varepsilon_0, K) 2^{-x_i/d} \tag{4}$$

Reducing equation (4) to an expression similar to that for incident radiation along the normal line, we have:

$$D_\gamma = a_\gamma b D_{\gamma 0} 2^{-h/d} \tag{4'}$$

Table 2. Coefficients α_1 (ψ, ε_0, K) in Consideration of Oblique Incidence

K \ tgφ	0	0.5	0.07	1.0	1.2	1.5	1.73	2.00	2.715
N_i	0	1.12	1.2	1.41	1.56	1.8	2.00	2.25	2.925
10^{-1}	1	1	1.00	1.00	1.00	1.00	1.00	1.05	1.20
10^{-2}	1	1	1.01	1.29	1.40	1.70	1.90	2.05	2.50
10^{-3}	1	1	1.03	1.72	2.00	2.50	3.50	4.10	5.60
10^{-4}	1	1	1.46	2.36	2.90	4.80	6.30	8.00	12.8
10^{-5}	1	1	1.80	3.40	4.30	8.30	11.4	15.4	26.5
10^{-6}	1	1.0	2.30	5.60	6.50	14.4	20.4	30.0	57.0
10^{-7}	1	1	3.20	7.40	10.0	21.9	36.4	62.0	132
10^{-8}	1	1	4.50	11.0	15.5	43.6	65.0	132	317
10^{-9}	1	1	6.60	17.4	24.0	76.0	116	211	770
10^{-10}	1	1	10.0	26.7	37.0	132	205	652	1880
10^{-11}	1	1	15.5	41.0	57.0	23.0	362	1500	4600
10^{-12}	1	1	24.4	75.0	88	402	642	3360	11200
10^{-13}	1	1	38.7	107	136	704	1140	8050	27200
10^{-14}	1	1	65.7	150	210	1240	20400	23000	65800

Remark

1. $N_i = \frac{1}{\cos\theta}$

   This table is based on Table 21 in the book "γ Radiation in an Atomic Explosion" and "uses" the horizontal protective layer.

2. The calculation of the attenuation of the dosage of penetrating radiation is obtained by extended computation of ψ.

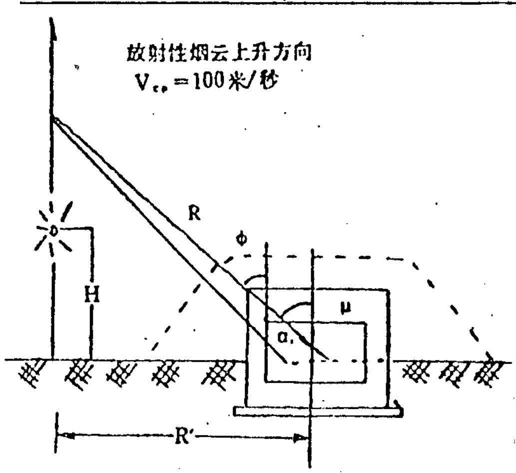

←Direction of rising smoke cloud
V_{cp} = 100 meters/second

Figure 2. αi: Oblique Angle
ψ: Incident Angle

where: d -- The half-value thickness of the material (Table 3).

b -- Coefficient of attenuation of oblique incidence,

$$b = \frac{1}{n} \sum_{i=1}^{n} a_i(\varphi \varepsilon_0 K) 2^{(H - x_i)/d},$$

Tables 4 and 5 list the coefficient of oblique attenuation of radiation released by an atomic bomb through concrete (reinforced concrete).

x_i -- Oblique thickness of the protective layer at different time intervals.

To the roof:

$$x_i = \frac{H_n}{\cos\varphi_i} = \frac{H_n\sqrt{(H + v_{cp}t_i)^2 + R'^2}}{H + v_{cp}t_i} \tag{5}$$

To the wall:

$$x_i = \frac{H_n}{\sin\varphi_i} = \frac{H_{CT}\sqrt{(H + v_{cp}t_i)^2 + R'^2}}{R'} \tag{6}$$

H_n -- Thickness of the protective layer of the roof (meter).

H_{CT} -- Thickness of the protective layer of the wall (meter).

H -- Altitude of explosion of the atomic bomb (meter).

R' -- Distance of underground structure from the point of projection of the center of explosion (meter).

ψ_i, ψ_{i-1} -- The angle between the incident γ radiation and the normal line of the protective layer in the interval t_i, t_{i-1}.

t_i, t_{i-1} -- represent time. The duration of irradiation by γ ray on the underground structure is divided into n segments, $t_i(t_{i-1})$ is the time passed between the beginning of the atomic explosion and the instant at the end of the i(i-1) interval. This period is about 15 seconds. The percentages of each dosage instantaneously released within the 15 seconds are listed in Table 6.

Table 3. Half-Value Thickness of Materials

Name of materials	Weight of unit volume (gram/centimeter)	Half-value weakening thickness d_n
Snow	/	50
Wood	0.7	30
Ice	1.0	23
Soil, sand	1.7	14
Weathered pebble, soft shale	2.0	12
Arenaceous shale, schistose sandstone	2.4	10
Granite, gneiss	2.7	10
Masonry	1.5	15
Concrete	2.8	10
Reinforced concrete	2.4	10
Iron	7.8	2.8

Table 4. Coefficient of Oblique Attenuation of Roof b

H_n/d_n \ R_1/N	0.5	1.0	1.5	2.0
8	0.710	0.390	0.220	0.14
15	0.500	0.250	0.090	0.065
20	1.460	0.200	0.061	0.052

Table 5. Coefficient of Oblique Attenuation of Wall b

$Hc\gamma/dn$ \ H/R_1	0.5	0.67	1.0	2.0
8	0.48	0.39	0.17	0.030
10	0.40	0.30	0.13	0.015
12	0.33	0.25	0.093	0.0067
15	0.30	0.19	0.61	0.0036
18.5	0.19	0.16	0.038	0.00071
20	0.18	0.12	0.033	0.00056

Note: Tables 3 and 4 are based on q equals 8,000 tons, H=400 meters in a mid-air atomic explosion. If q is greater than 8,000 tons, using the numerical values in the tables is safer.

Table 6. Doses of Radiation Instantaneously Released by Mid-air Explosion of an Atomic Bomb

Types of protective layer	To the wall					To the roof				
辐射设百分比 均算时间(秒) (2) (1)当量 (千吨) 辐射百分比% (3)	8	20	30	150	5000	8	20	30	150	5000
0—20	0	0	0	0	0.4	0.025	0.03	0.04	1.35	2.2
20—40	0.025	0.03	0.40	0.35	2.2	0.13	0.16	0.28	1.2	3.8
40—60	0.13	0.16	1.28	1.2	3.8	0.55	0.7	1.0	30	50
60—80	0.55	0.7	1.0	3.0	5.0	2.0	2.3	3.0	5.0	7.5
80—100	2.0	2.3	3	5	7.5	15	15	15	15	20

Key: (1) Equivalent (1,000 tons)
(2) Radiation in percentage all calculated in time (second)
(3) Percentage of radiation

III. Example of Calculating the Protection of Air Raid Shelters From γ Ray

We have an attached air raid shelter (building with 6 floors, height of each floor is 3.2 meters). The equivalent power of the atomic bomb is 8,000 tons, the altitude of explosion is 400 meters, the explosion occurs to the side in the rear of the air raid shelter. The structure is R' = 400 meters from the point of projection of the center of explosion. Verify the ability to protect against γ radiation.

1. Consider the mid-air explosion effect to calculate the incident dose of γ radiation:

The computational formula: $D_{\gamma 0} = AK/R^2$ (7)

where: K -- the correlation coefficient of equivalent power q of the atomic bomb

A -- Considering the density ρ of mid-air explosion, the coefficient of the effect of C type photon energy.

From the distribution of the doses of γ radiation (Figure 3) from the explosion of the atomic bomb over Hiroshima, we can obtain the following simplified formula:

When $R < R_1$, $A = 1$

When $R_1 \leqslant R \leqslant R_2$, $A = e^{-R/250}$

According to some reference works, at this time $A = e^{-R/300}$

From the concept of physics in the study of the effects of shock waves, O.I. Leipunski gives:

$$\text{Mid-air explosion:} \quad K = 6.6 \times 10^{8} q e^{(0.925\sqrt[5]{q} - 6.25 \times 10^{-5} q)} \tag{8}$$

Further simplifying equation (8) gives us:

$$K = 1.4 \times 10^{9} q(1 + 0.2q^{0.65}) \tag{8'}$$

At this time, the value of K can be found in Figure 4.

Ground explosion:

$$K = 2.8 \times 10^{9} q(1 + 0.3q^{0.65}) \tag{9}$$

When $R > R_2$, $A = e^{-R/393}$

$$K = 5.5 \times 10^{8} q[1 + 0.05(aq)^{0.5}] \tag{10}$$

or simplified as $K = 5.5 \times 10^{8} q$ (10')

Ground surface explosion a = 2, mid-air explosion a = 1.

R - Distance of air raid shelter from center of explosion.

$R = \sqrt{H^2 + R'^2} = \sqrt{400^2 + 400^2} = 565$ meters.

This problem belongs to $R_1 \leqslant R \leqslant R_2$ $A = e^{-R/250} = e^{-565/250} = 0.208$

From Figure 4 we obtain $K = 1.8 \times 10^{10}$

The incident dosage $D_{\gamma 0} = \frac{18 \times 10^{10}}{565^2} \times 0.208 = 10700$ roentgens

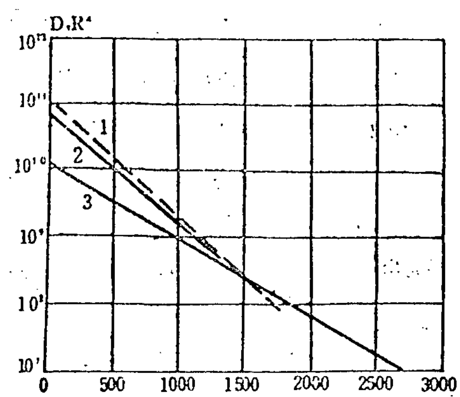

Figure 3. Experimental Data on the Distribution of the Doses of γ Radiation at Time of Explosion of the Atomic Bomb Over Hiroshima: 1. γ = 252 meters; 2. γ = 282 meters; 3. γ = 393 meters.

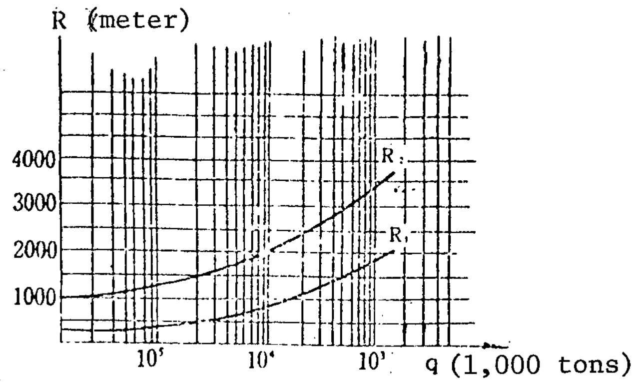

(I)

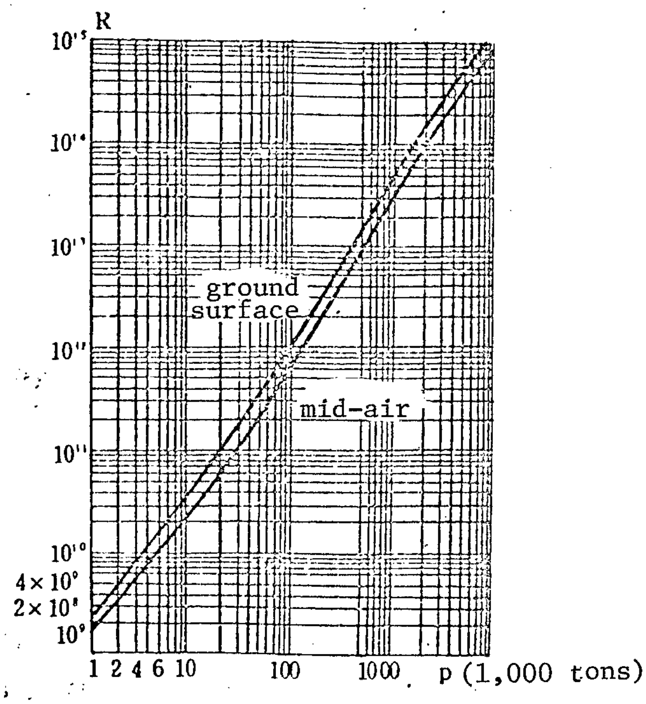

(II)

Figure 4. (I) R_1, R_2; (II) Rq Graph

2. The Attenuated Dosage of γ Ray When Passing Through the Roof of the Underground Air Raid Shelter

According to the actual situation, the incident γ ray is oblique. It first passes through the walls and the floors of the building, and then through the roof of the underground chamber and finally enters the underground chamber.

The computational formula: $D_\gamma^n = \alpha_\gamma b D_{\gamma 0} 2^{-H_n/d}$ (11)

From Figure 1 we find $\alpha_\gamma = 0.95$

From Table 4 we find R'H = 1, b = 0.39

We then convert the covering layer of furnace cinder of 10 centimeters thick to an equivalent thickness of reinforced concrete

$$H_w' = \frac{x\mu'}{\mu} = \frac{10 \times 0.027}{0.07} = 3.9 \text{ centimeters,}$$

and convert the thickness of the wall of two bricks thick into an equivalent thickness of reinforced concrete

$$H_{w''} = \frac{49 \times 0.05}{0.07} = 35 \text{ centimeters,}$$

and because the incident γ ray is oblique, therefore the wall thickness $H_{n9} = \frac{35}{\cos 45°} = 49.5$ centimeters. A six story building is on top of the underground chamber. It is possible for the γ ray to pass through five stories and reach the roof of the shelter. Therefore, its total thickness is $H_W = 10x5+3.9+30+49.5=133.4$ centimeters (note: The thickness of the floor of each story is 10 centimeters, the thickness of the roof of the underground chamber is 30 centimeters).

The dosage after attenuation:

$$D_\gamma^n = 0.95x0.39x10700x2^{-133 \cdot 4/10} = 0.38 \text{ roentgens.}$$

3. Dosage of Attenuated γ Ray After Passing Through the Wall Computational Formula: $D_\gamma^{CT} = a_\gamma b D_{\gamma 0} 2^{-H_{CT}/d}$ (12)

The wall of the underground air raid shelter is usually underground. On the walls of the semiunderground shelter and the pile type air raid shelter are exposed above ground. In this example, this portion will be neglected.

4. Attenuation of γ Ray by Holes

(1) Dosage of Incident Radiation Calculated According to the Theory of Angular Distribution

Experiments show that when a portion of the dosage of radiation is blocked by a shield and the radiation incident on the radiation detector is only the γ ray emerging from a scattering medium within a definite solid angle, the problem of angular distribution of radiation emerges. It can be seen that the γ ray through a hole can be regarded as entering according to a definite solid angle.

The computational formula: $D_{\gamma 1} = D_{\gamma 0} \cdot F(\theta) \cdot \Omega$ (13)

Related conference works state that the angular distribution function of the intensity of scattering of γ radiation in air from fission fragments can be written as

$$F(\theta) = K_{\alpha} \, [0.0092 + 3.22e^{(0.089\theta)}] \tag{14}$$

The angular distribution of the dosage of captured γ radiation obeys

$$F(\theta) = K_{\alpha} \, (0.008 + 2.11e^{(0.0659\theta)}) \tag{15}$$

$F(\theta)$ is the dosage of that component in the direction of the scattering angle θ and within the unit solid angle as a ratio of the total dosage of that component. θ is measured from the line linking the source and the detector.

K_{α} is the normalization coefficient and is related to α (the angle between the ground surface and the direction of the center of explosion) and the reflective property of the soil.

$$K_{\alpha} = \frac{\overline{K}_{\alpha}}{1 + A_{\gamma 0}(\alpha)}$$

$\overline{K}_{\alpha}$ is the normalization coefficient when the ground is taken as an absolute black medium that does not reflect γ radiation.

$A_{\gamma 0}$ (α) is the rate of the soil's integrative mirroring of γ radiation when the azimuth of the point of explosion is α.

The major portion of the captured γ radiation is already emitted within 0.1 second. Its action actually ends within 0.3 second after the explosion. During this time, the smoke cloud actually has not risen, therefore the source of the captured γ radiation, like the neutron source, can be regarded as a stationary source.

The dosage of γ radiation from fragments varies with time. It is determined by three factors, radioactive decay of the fragment itself, rising of the smoke cloud and the cavity formed by the shock wave in the atmosphere.

The dosage of γ radiation within a unit solid angle is:

$$D(\theta, \varphi) = \frac{\int_0^{t_k} K_a^f(t)[0.0092 + 3.32e^{-0.038\theta(t)}] \, u(t)K_{\gamma}(t)K_H(t)dt}{\int_0^{t_k} u(t)K_{\gamma}(t)K_H(t)dt} \tag{16}$$

while $$\theta(t) = \arccos\left[\sin\left(\operatorname{arctg}\frac{H+16t^2}{\sqrt{R^2-H^2}} - \alpha\right)\sin\theta\cos\varphi + \cos\left(\operatorname{arctg}\frac{H+16t^2}{\sqrt{R^2-H^2}} - \alpha\right)\cos\theta\right] \quad (17)$$

In actual application, this formula is too cumbersome. To satisfy the needs in engineering computation, we suggest using the following formula for calculations.

Computational formula: $D_{\gamma 2} = D_{\gamma 0}\eta_\gamma \Omega$ (18)

where:

$D_{\gamma 2}$ -- Dosage of radiation entering the hole (roentgen).

When η_γ-----Ω = 1, the ratio between the dosage of radiation entering the hole and the dosage of total radiation can be found in Figure 5.

Ω -- The solid angle of the hole, $\Omega = a/r^2$.

a -- The sectional line of the solid angle of the hole.

r -- Radius of the solid angle (centimeter).
Radius (centimeter).

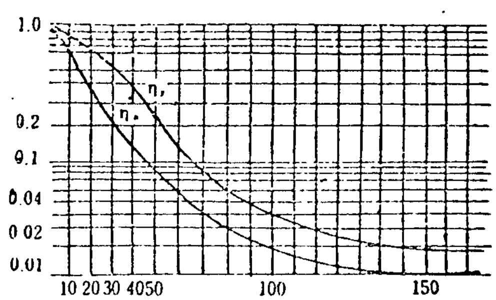

Figure 5. Ratio Between the Dosage of Radiation Entering the Hole and the Dosage of Radiation Incident on the Entire Outer Layer of the Fortification

Now let us explain the computational process according to the conditions given in the above example.

Because of the rise of the smoke cloud after an atomic explosion, each instantaneous solid angle and the azimuth of the center of explosion change, i.e., the angle $\psi' = \psi_1 + 90°$ (ϕ_1 - the instantaneous incident angle). We know from the diagram that as the angle ϕ' changes, the ratio η_γ also changes correspondingly.

According to the conditions given in this problem, when

the radiation is 0 to 20 percent, $\phi' = 45° + 90° = 135°$, $\eta_1 = 0.017$,
the radiation is 20 to 40 percent, $\phi' = 135°$, $\eta_2 = 0.017$,
the radiation is 40 to 60 percent, $\phi' = 44° + 90° = 134°$, $\eta_3 = 0.019$,
the radiation is 60 to 80 percent, $\phi' = 40° + 90° = 130°$, $\eta_4 = 0.020$,
the radiation is 80 to 100 percent, $\phi' = 32° + 90° = 122°$, $\eta_5 = 0.022$.

$\Omega = s/r - 2x180+2x110 \div 400^2 = 0.058$

D_{r2} = 10700x0.058(0.017+0.017+0.19+0.020+0.022)/5=11.79 (roentgens)

(2) The Dosage of Incident Radiation Calculated According to the Coefficient of Attenuation

The C type ray transmitted from the center of explosion to the underground structure moves in a straight line. When it passes through the hole, it must turn a right angle. This will weaken the dosage of radiation. The coefficient of attenuation introduced in currently available data varies. (U.S.) anti-atomic engineering references believe that this can weaken the radiation by 0.07 times. Some data state this can weaken it by 0.25 times. This is because when the radiation enters a horizontal passageway, the difference between the passageway and the section of the entrance will further weaken the radiation. This weakening effect is generally called an added effect or area effect. The transmission coefficient AF_a of the area effect can be expressed by the following formula.

$$AF_a = \frac{\text{Area of horizontal entrance}}{\text{Area of section of horizontal passageway}} \quad (19)$$

Radiation enters the underground air raid shelter through a horizontal passageway possesses a similar area effect expressed by the formula:

$$AF'_a = \frac{\text{Area of section of horizontal passageway}}{\text{Area of section of underground chamber}} \quad (20)$$

Undoubtedly, when radiation passes through the protective door, the intensity of radiation is further weakened. Due to a lack of data, we temporarily suggest using a transmission coefficient of 0.92, i.e., the intensity $D_{\gamma 3}$ of the C type radiation:

$$D_{\gamma 3} = D_{\gamma 0} \times AF_a \times AF'_a \times \text{transmission coefficient of turning}$$
$$\times \text{ transmission coefficient of the door}$$

Calculations based on the conditions of this problem are as follows:

We know: The area of the entrance is 90 x 160
The area of the section of the passageway is 200 x 240
The area of the section of the underground chamber is 240 x 600
(referring to a room in the underground chamber)

a. Now considering turning three right angles, the incident dose is:

$$D_{\gamma 3}' = 0.07^3 \times 10700 = 3.67 \text{ roentgens}$$

b. $AF_a = \dfrac{1.0 \times 1.7}{2.0 \times 2.4} = 0.35$

c. $AF_a' = \dfrac{2.0 \times 2.4}{2.4 \times 6.0} = 0.33$

d. The dosage of radiation after being attenuated by passing through reinforced concrete of 10 centimeters thick:

$$D_{\gamma 3}'' = a_\gamma \times D_{\gamma 3}' 2^{-h/d_0} = 0.95 \times 3.67 \times 2^{-10/10}$$

$$= 1.75 \text{ roentgen}$$

The dosage entering the hole is:

$$D_{\gamma 3} = D_{\gamma 0} \times AF_a \times AF'_a \times \text{transmission coefficient of turning} +$$

$$D_{\gamma 3''} = 10700 \times 0.35 \times 0.33 \times 0.07^3 + 1.75 = 2.17 \text{ roentgens}$$

e. The dosage of γ ray entering the underground chamber:

$$D_\gamma = 0.38 + 11.79 + 2.17 = 14.34 \text{ roentgens}$$

IV. Calculation of the Protection of an Air Raid Shelter Against Neutron Stream

1. Calculating the Incident Dosage D_{n0} of Neutron Stream

$$D_{n0} = (m/R^2)(e^{-R/250}) \text{ (Biological roentgen - equivalent)} \quad (19)$$

where: m -- is determined by the coefficient of the equivalent power of the atomic bomb, according to Figure 7.

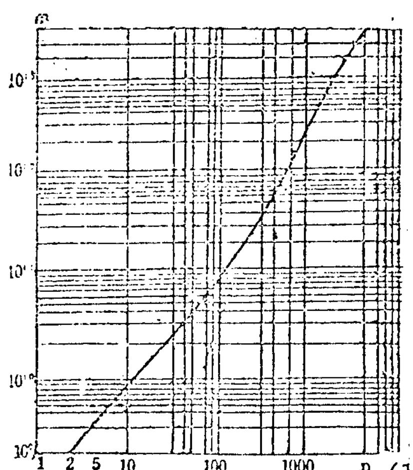

Figure 7. q-m diagram

$$D_{n0} = \frac{4 \times 10}{565} e^{-565/250}{}^{9} = 12500 \text{ (biological roentgen-equivalent)}$$

2. Calculating the Dosage After Being Attenuated by Passing Through the Roof When the Incident Neutron Stream Is Oblique

Computational formula: $D_n = a_n D_{n0} 2^{-H_n X / d_{n} \cos\phi}$ (20)

where: D_n -- the dosage of neutron stream after passing through a roof of thickness $\frac{H_n X}{\cos\phi}$;

d_{n0} -- half-value thickness of neutron stream, see table.

a_n -- considering the attenuation coefficient of neutrons effected by the surface of the medium, found in Table 8.

Table 8.

Name of material	dnn half-value attenuation thickness	an
Soil, masonry	12	0.7
Concrete	11.6	0.6
Steel	6	0.25

(1) Convert the floors, walls and furnace cinder into equivalent thickness of reinforced concrete.

Furnace cinder of 10 centimeters: $H'_{n9} = \frac{10 \times 9.7}{11.6}$ = 8.4 centimeters

Wall: $H''_{n9} = \frac{49 \times 12}{11.6}$ = 50.7 centimeters

Floors: H'''_{n9} = 5 x 10 = 50 centimeters

The roof of the underground chamber is 30 centimeters

The total thickness of the roof H_n = 8.4 + 50.7 + 50 + 30 = 139 centimeters

(2) $\cos\phi = \frac{400}{\sqrt{400^2 + 400^2}} = 0.71$

(3) Dosage after attenuation:

$$D_{n1} = 0.6 \times 12500 \times 2^{-139/0.71 \times 11.6} = 0.062 \text{ (biological roentgen-equivalent)}$$

2. Calculating the Dosage After Being Attenuated by Passing Through the Wall When the Incident Neutron Stream Is Oblique

Computational formula: $D_{n2} = a_n D_{n0} 2^{-H_{cm}/\sin\phi\, d_n}$ (21)

Because the underground chamber is underground, this portion of the incident dosage is overlooked.

3. Dosage of Neutron Stream Entering Through the Door After Being Attenuated

(1) Calculating the dosage of neutron stream entering the door according to angular distribution

Computational formula: $D'_{n2} = D_{n0}\eta_n \Omega$ (22)

Let the vertex of the solid angle be the central point between two passageways, take r=120 centimeters, the angle in between $\phi'=135°$, from Figure 5 we find $\eta_n = 0.012$, s = 2x110+2x180=580 centimeters,

$$\Omega = \frac{580}{120^2} = 0.04$$

$$D'_{n3} = 12500 \times 0.012 \times 0.04 = 6 \text{ (biological roentgen-equivalent)}$$

(2) Dosage of neutron stream being attenuated by passing through the protective door

Computational formula $D_{n2} = a_n D'_{n3} \cdot 2^{-h/d_n}$

$$= 0.6 \times 6.0 \cdot 2^{-10/11.6} = 1.98$$

(biological roentgen-equivalent)

4. Total Dosage of Neutron Stream Entering Underground Chamber

$$D_n = 0.062+0+1.98=2.042 \text{ (biological roentgen-equivalent)}$$

5. The Sum of the Total Residual Dosage of γ Ray and Neutron Stream Found by the Above Steps Must Not Surpass the Allowable Dosage of 50 Roentgens

$$\text{i.e., } D = D_\gamma + D_n = 14.34 + 2.042 = 16.382 < [50]$$

V. Characteristics of Calculating the Penetrating Radiation From an Explosion of Thermonuclear Weapons

As described above, the presence of ultrahigh velocity neutrons is the characteristic of penetrating radiation from an explosion of thermonuclear weapons. For the various types of hydrogen bombs, γ ray still constitutes the major component of radiation. The proportion of fast neutrons and ultrahigh velocity neutrons generally is not large and ordinarily they can be calculated according to the following formulas:

Dosage of γ ray: $D_\gamma = \frac{4 \times 10^{13}}{R^2} e^{-R/250}$ (roentgen) (23)

Dosage of fast neutrons: $D_n = \frac{3 \times 10^{12}}{R^2} e^{-R/250}$ (biological roentgen-equivalents) (24)

Dosage of ultrahigh velocity neutrons: $D_{ultra} > \frac{4 \times 10^{11}}{R^2} e^{-R/250}$

(biological roentgen-equivalent) (25)

VI. Conclusion

By the above discussion, we have gained an understanding of the calculation of penetrating radiation incident on fortifications. We have cited the following points and we invite the reader's attention to avoid mistakes.

1. This article assumes that the rise of the smoke cloud from a nuclear explosion is of even velocity, i.e., $H_t = H + \nu_{cp}t$ (ν_{cp} = 100 meters/second). Assistant Professor Qian Shihu [6929 1102 5706] told us that the book by Kukhotavich(?) et al. (USSR) entitled "Protection Against Neutron Stream and Radiation in Nuclear Radiation" states that the rise of the smoke cloud is of even acceleration, i.e., $H_t = H + 6t^2$. Because recent English and American publications do not have such descriptions, the above article was not revised. This is specially explained here.

2. This article considers the smoke cloud to rise at an even velocity, therefore the incident dosage is calculated according to equation (3). If it rises at evenly variable velocity, then at this time, the incident dosage becomes a variable and we can use integration to find the value of $D_{\gamma 0}$. If there are actually measured data, such data could be directly used.

3. When considering the rise of the smoke cloud at an even acceleration, we could still approximately take the numerical values listed in Tables 4 and 5. When considering even acceleration, the table of oblique attenuation coefficients of the protective layer will have to be compiled by the authors.

Because of the lack of in-depth knowledge of the authors and the limited level of knowledge, there will be some mistakes in this article. It is hoped that experts, scholars and the broad number of readers will point them out.

REFERENCES

1. O.N. Leipunski, translated by Tang Bi [0781 3968]: "γ Radiation in Atomic Explosions," China Industry Press, 1963.

2. Chen Shuhui [7115 2885 1798]: "Calculation of the Weakening of Penetrating Radiation by Horizontal Protective Layers," "People's Engineer," 1963, additional issue No 33.

3. J.R. Lamarhi: "Introduction to Nuclear Engineering," London, 1975.

4. A. Edwardprofio: "Radiation Shielding and Dosimetry," New York, 1979.

5. Kang Ning [1660 1337]: "Calculation of the Protection of Fortifications Against Penetrating Radiation," "People's Engineer," 1963, additional issue No 33.

9296
CSO: 4013/15

BRIEFS

PROCESS FOR VANADIUM RECOVERY--Beijing, 22 Jan (XINHUA)--Chinese scientists have developed a new process for the treatment of molten iron containing precious vanadium. "The process will help open new prospects for the multiple use of the iron ores from Panzhihua," the Chinese Academy of Sciences said here today. Panzhihua, on the Jinsha River in the south-western part of Sichuan, southwest China, has one of the world's largest deposits of vanadium-titanium magnetic iron ore containing cobalt, nickel, chromium, gallium and other elements. China had developed several methods to recover iron, vanadium and titanium. "But this process is much better," the academy added. The academy said that the new process will help solve several key problems in iron and steel smelting and recovery. The process is also conducive to raising the production capacity of blast furnaces and converters and steel quality and increasing the varieties of iron and steel. Scientists and technologists of the Panzhihua Iron and Steel Research Institute and the academy's Institute of Chemical Metallurgy recently carried out a semi-industrial experiment of this new process in Xichang, Sichuan Province, the academy said. [Text] [OW221004 Beijing XINHUA in English 0711 GMT 22 Jan 83]

CSO: 4010/36

HOSPITAL PROVIDES FREE TREATMENT TO TIBETANS

OW240829 Beijing XINHUA in English 0711 GMT 24 Jan 83

[Text] Lhasa, 24 Jan (XINHUA)--A People's Liberation Army hospital here has provided free medical treatment for an average of 6,000 Tibetan civilians including 200 inpatients annually, a spokesman of the hospital told XINHUA.

While attending to military personnel in the capital of the Tibet Autonomous Region, the hospital regularly sends medical teams to tour nearby villages and residential areas where they treat diseases and give medical check-ups for all people free of charge. The PLA doctors have helped local peasants establish clinics and trained medical workers for them.

Medical personnel from the hospital have made a point of organizing first-aid teams to help the peasants during harvest time, with hospital technicians helping repair farm tools.

The hospital has been particularly successful in treating mountain sickness, and the medical staff has written a manual on the prevention of this ailment. Experience over the years shows the hospital's cure rate for plateau pulmonary cedema, a disease with the highest death rate in Tibet, has reached 99 percent.

Recently, an elderly Tibetan peasant named Gyaincain, who had fallen into a coma after suffering massive hemorrhage in the alimentary canal, was brought to safety and fianlly restored to health after 3 months' treatment in the hospital, which not only provided him with medical care but also nutritious food free of charge.

On occasions of the Tibetan new year, local people would come to the hospital with buttered tea and fried cakes and extend their greetings to the doctors and nurses.

CSO: 4010/35

SICHUAN SCIENCE COMMENDATION MEETING OPENS

HK210257 Chengdu Sichuan Provincial Service in Mandarin 2300 GMT 20 Jan 83

[Summary] A Sichuan provincial science and technology commendation meeting opened in Chengdu on 20 January. Provincial CPC Committee Deputy Secretary and Acting Governor Yang Xizong presided. Present at the opening ceremony were Nie Ronggui, Lu Dadong, Du Xinyuan, Liu Xiyao, Ren Baige, Wu Xihai, (Song Daban), (Jiang Mingkuan), (Gu Jinchi), (Liu Chunfu) and (Kong Cheng), responsible comrades of the provincial CPC Committee, People's Congress Standing Committee, government and CPPCC, the Chengdu PLA units and Sichuan Military District. The provincial leaders presented awards and citations to the participants.

Provincial CPC Committee Secretary Yang Rudai made a speech. After greeting the participants and congratulating them on their achievements, he pointed out: The main reasons why the province's science and technology work could score such great successes in only a few years are, first, the province's scientific and technical workers have the strong aspiration to change China's backward state and build a prosperous, rich and strong modern socialist motherland. Second, the province's scientific and technical workers have geared their work to economic construction and linked it to the province's industrial and agricultural production. The results of their researches have been rapidly popularized in production and yielded outstanding economic results. Third, the province's scientific and technical workers have closely cooperated with and supported each other. They have also worked with the masses to create various organizational forms linking scientific research with production.

CSO: 4008/41

BRIEFS

OFFICIALS ATTEND MEDICAL FORUM--The China Association for Science and Technology sponsored a new year forum for the China Medical Society at the Great Hall of the People today. Attending the forum were Zhou Peiyuan, chairman of the China Association for Science and Technology, Cui Yueli, minister of public health, Qian Xinzhong, chairman of the State Family Planning Commission and honorary president of the China Medical Society, as well as nearly 400 medical specialists, professors and middle-aged medical personnel in the capital. At the forum, noted medical scientists Zhong Huilan, Wu Ruiping, Deng Jiadong, Wu Jieping, Ye Gongshao and Yan Renying enthusiastically discussed the improvement and development of medical work with various medical specialists. [Text] [OW260851 Beijing Domestic Service in Mandarin 1200 GMT 23 Jan 83]

YANG XIZONG ON SCIENCE, TECHNOLOGY--Sichuan Provincial CPC Committee Deputy Secretary and Acting Governor Yang Xizong delivered a report at the provincial science and technology commendation gathering on 21 January. Provincial CPC Committee Standing Committee member and Vice Governor He Haoju presided at the gathering, which adopted a letter of proposal on learning from Comrades Jiang Zhuying and Luo Jianfu. After extending greetings and congratulations to the participants and to scientists and technicians throughout the province, Yang Xizong gave his views on the following matters: "1) Enhance understanding of science and technology and rely on progress in science and technology to quadruple total annual industrial and agricultural output value; 2) readjust the structure of technology and reform the science and technology setup; 3) implement the party's principles and policies and implement the fruits of scientific research in production." [Summary] [HK220311 Chengdu Sichuan Provincial Service in Mandarin 2300 GMT 21 Jan 83]

CSO: 4008/41

AUTHOR: SHI Wang [2514 2598]

ORG: None

TITLE: "XWT-S Small Table Model Display Recording Instrument"

SOURCE: Beijing YIQI YU WEILAI [INSTRUMENTATION AND FUTURE] in Chinese No 10, 1982 p 18

ABSTRACT: Shanghai Automation Instrument and Meter Plant No 3 succeeded in making the XWT-S small table model display recording instrument. It represents a new series of display recording instruments in China. Its precision is rated as 0.5 grade [?] and its stroke is less than 1 sec. The range of measurement may be changed seven different ways and the speed of movement of the recording paper may also be varied seven different steps (to a maximum of 100 mm/sec.) DC amplification (integrated circuits) is adopted to realize speed feedback inside the amplifier so that the circuit is simple and the instrument is stable and reliable. When the range is being changed, the input impedance of the instrument does not alter. The range of display may be regulated from 20 to 100 percent and the zero shift may be continuously adjusted within the measurement range of -50 to 100 percent [?]. The recording paper is driven by a stepper motor so that the speed variation is large, the structure is tight, and the noise is small.

AUTHOR: LIU Ke [0491 4430]

ORG: None

TITLE: "Research for Making W_2 Laser Facular Camera Succeeded"

SOURCE: Beijing YIQI YU WEILAI [INSTRUMENTATION AND FUTURE] in Chinese No 10, 1982 p 18

ABSTRACT: Most recently, the W_2 laser facular camera was successfully made by Beijing Research Institute of Photographic Machinery and Shanghai Research Institute of of Ship Transportation, as a joint research project to create this new equipment for China's research studies in experimental mechanics. This is an instrument of precision measurement utilizing laser facular interference to obtain total information and to achieve no-contact measurement. It can proceed to measure deformation, displacement, vibration, and other factors of mechanics of a structure under dynamic, static, high temperature, and other conditions. The instrument is composed of the 3 components of the facular camera, the point by point analyzer, and the optical information processor. First, laser is used to illuminate the part of the object to be studied. The facular camera is used to record the changes of that part onto the high resolution film, which is then placed in the analyzer to measure the variables point by point. The film may also be placed in the optical information processor to obtain the variables at once through a wave filter. The electronic shutter speed of the instrument is 0.5-100 sec; the scanning range of the facular picture is 80 x 110 mm^2; the size of the facula on the picture is 0.5 mm.

6168
CSO: 4009/51

AUTHOR: HONG Zhiguang [3163 1807 0342]

ORG: None

TITLE: "Error Indicator Regulating Instrument"

SOURCE: Beijing YIQI YU WEILAI [INSTRUMENTATION AND FUTURE] in Chinese No 11, 1982 p 12

ABSTRACT: Most recently, Shanghai Automation Instrument and Meter Plant No 6 succeeded in making the error indicator regulating instrument for the TES series temperature controller, which may be directly installed on light industry machines. This instrument is also suitable for metallurgical, petrochemical, chemical fiber, and electrical power industries. This instrument comes in the following types: the 2-digit type, the 3-digit type, the time ratio type, the continuous PID type, and the pulse PID type. It may also be coordinated with thermocouples, thermal resistors, and related transmitting and transforming devices. The regulator is simple in structure, reliable in operation, convenient to maintain and repair, small in size, and easily installed. It is currently being tested by such units as Shanghai Tobacco Plant and has been found to be satisfactory. It will be available in the marketplace before long.

AUTHOR: GU Xiwen [7357 6932 2429]

ORG: None

TITLE: "Direct Current Stable Voltage and Stable Current Power Source"

SOURCE: Beijing YIQI WEILAI [INSTRUMENTATION AND FUTURE] in Chinese No 11, 1982 p 12

ABSTRACT: Most recently, Shanghai Huguang Instrument Plant succeeded in making the YJ63 stable voltage and stable current DC power source. It has high stability (5×10^{-5}) and low internal resistance (below 0.5 mΩ) and can output stable voltage power, adjustable for 0-50V continuously. It can also output stable current power of high stability (5×10^{-5}) and high internal resistance (above 100 kΩ) and adjustable for 0-5 A. This power source is suitable for electronic equipment, automatic control devices, and measuring instruments. In either series or parallel connection, this power source may provide output amplification in multiples of either voltage or current. As the load resistance varies from 0 to infinity, the electric power can automatically transfer to either stable voltage or stable current state to guarantee high stability of the load voltage. This power source also has remote sampling capability and can remove voltage drop error of the connecting wire.

6168
CSO: 4009/59

AUTHOR: LIU Yanzhu [0491 1693 2691]

ORG: Shanghai Jiaotong University

TITLE: "Coupled Motion of Gimbal Gyroscope and Spin Satellite"

SOURCE: Beijing LIXUE XUEBAO [ACTA MECHANICA SINICA] in Chinese No 6, 1982 pp 570-577

TEXT OF ENGLISH ABSTRACT: The coupled motion of a gimbal gyroscope and a spin satellite is treated by the perturbation method. The state of motion of the system of four rigid bodies is described by the phase coordinates and the perturbation equations are established. The inertial torques of the gimbals are regarded as perturbations to Euler-Poinsot motions of the gyro and the satellite. The formula of the rate of the coupled nutation drift of the gyro and satellite is derived, and the well-known Magnus' formula is a special case when the satellite has no nutation. The phenomenon of exchange of the modulus of angular momentum between the gyro and satellite can occur for the synchronous nutation, when the gyro and satellite have equivalent nutation frequencies. The stability criteria of the coupled nutation damping motion of the gyro and satellite caused by viscous friction in the bearings are obtained. The well-known stability criterion for a symmetrical rotor in viscous medium and the stability criterion for a spin satellite with internal energy dissipation are two special cases of the stability criterion for the coupled nutation damping motion.

AUTHOR: WANG Songgao [3769 2646 4108]

ORG: Institute of Mechanics, Chinese Academy of Sciences

TITLE: "Some Problems in the Design of the Tube Wind Tunnel"

SOURCE: Beijing LIXUE XUEBAO [ACTA MECHANICA SINICA] in Chinese No 6, 1982 pp 570-577

TEXT OF ENGLISH ABSTRACT: The problem of the boundary layer growth in the charge tube is discussed. An analytical solution is derived and has been reduced to an algebraic expression. The result contains various factors which affect boundary layer growth. The calculation is simple and the results coincide with those of experiments.

Based on F.L. Shope's model, analytical expressions for the test section starting process are derived. Various factors which affect the starting process are analyzed. The precision of calculation is enough for design purposes. The calculating procedure is much simpler than that of F.L. Shope.

9717
CSO: 4009/67

AUTHOR: XU Shimin [1776 0099 2404]

ORG: Research Institute of Hoists and Conveyances, Ministry of Machine Industry

TITLE: "YLK-480 and YOT-400 Hydraulic Coupling Devices Certification Conference"

SOURCE: Beijing QIZHONG YUNSHU JIXIE [HOISTS AND CONVEYANCES] in Chinese No 12, 6 Dec 82 p 64

ABSTRACT: The certification conference sponsored by Bureau of Basic Devices of Ministry of Machine Industry was held in Shanghai, 11-13 Oct, and attended by 55 delegates of 33 units, including Ministries of Machine Industry and Metallurgy, Academy of Designing, Shanghai Municipal Bureau of Metallurgy, etc. The delegates listened to reports on the research process of the devices, the research on high strength aluminum alloy, and the applications of the devices to the converter fan systems and reviewed related technical documentations. An inspection tour was conducted by the delegates at Shanghai Steel Mills No 1 and No 2 to observe the hydraulic coupling devices in operation. They concluded, unaniously, that the industrial experiments of more than 3 years at these mills have proved that the coupling devices, designed to be used with 15-30 and 50 ton converter fan systems, produce obvious economic benefits of prolonging equipment life and increasing steel production and they should be produced in batches. The delegates also hoped that Ministries of Machine Industry and Metallurgy would vigorously extend such devices for the purpose of contributing to energy conservation.

6168
CSO: 4009/69

END